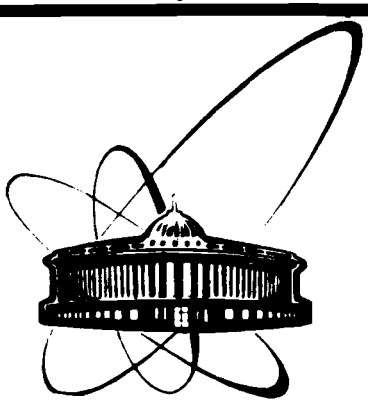

Объединенный
институт
ядерных
исследований
дубна

E17-89-538

W.Salejda *

THE VIBRATIONAL SPECTRA OF THE ONE-DIMENSIONAL HARMONIC MODEL OF THE QUASIPERIODIC BINARY ALLOY

Submitted to "Acta Physica Polonica"

* On leave of absence from Institute of Physics, Technical University of Wroclaw, Wybrzeze Wyspianskiego 27, 50-370 Wroclaw, Poland

1989

1. Introduction

In the earlier paper [1], hereafter called I, the numerical results of the detailed studies of the vibrational spectra (VS) of the one-dimensional Fibonacci quasicrystals (1D FQ) have been reported. It has been assumed in I that: (1) the masses of atoms are identical and (2) the force constants $k_{l,l+1}$ and $g_{l,l+2}$ of the nearest-neighbour (NN) and next-nearest-neighbour (NNN) interactions of atoms, respectively are given by the binary quasiperiodic sequences

$$k_{l,l+1} = k_0 \{ 1 + q (1 - d_{l,l+1}) \} \qquad (1)$$

$$g_{l,l+2} = g_0 \{ 1 + q (2 - d_{l,l+2}) \}, \qquad (2)$$

where

$$d_{l,l+i} = [(l + i) / \tau] - [l / \tau] \qquad (3)$$

$$i = 1 , 2 .$$

are the distances between NN and NNN atoms, [x] denotes the integer part of x, τ is the golden ratio and q is the so-called parameter of quasiperiodicity (POQ).

In continuation of I, the lattice dynamics of the one-dimensional crystal containing two types of atoms that are quasiperiodically distributed along the chain will be discussed. The considered model of the one-dimensional quasicrystals is more realistic than the system investigated in I since, as has been shown by Burkhov [2], the concept of quasicrystalline state [3-5] in the one-dimensional case can be used to describe the binary chain of atoms and is inapplicable to the pure chain (nevertheless cf. 8th conclusion in Sec.5).

The aim of the present paper is to study the properties of VS

of the one-dimensional harmonic model of quasiperiodic binary alloy (QBA).

The proposed model describes the dynamics of the pure (periodic $q = 0$) and quasiperiodic binary ($q > 0$) chain of atoms.

The NNN interactions of atoms are taken into account and the detailed numerical studies of the structure and fractal dimension of VS will be performed under free end boundary conditions (FEBC) in a wide range of the model parameters.

The paper is organized as follows. In Sec.2 the specification of the model is given. In Sec.3 the basic system of equations is derived. The numerical results are presented in Sec.4. Sec.5 contains the main conclusions.

2. Specification of the model

The quasilattice (QL) of the one-dimensional quasiperiodic binary alloy (1D QBA) is defined by [2-5]

$$x_n = n + \beta + [\, n/\tau + \alpha \,] / \tau, \qquad (4)$$

where α and β are the real numbers; n is an integer number.

We decorate QL (4) placing n-th atom having the mass

$$M_n = M_0 \, (\, 1 + q \, ([(n+1)/\tau] - [n/\tau])) \qquad (5)$$

halfway between x_{n+1} and x_n (see Fig.1) i.e., the equilibrium coordinate l_n of n-th atom is

$$l_n = (\, x_{n+1} + x_n \,) / 2 \, . \qquad (6)$$

Let us recall that the quantity $q = z / \tau$ appearing in (5) is the parameter of quasiperiodicity [1].

The interactions of atoms in the model under consideration are

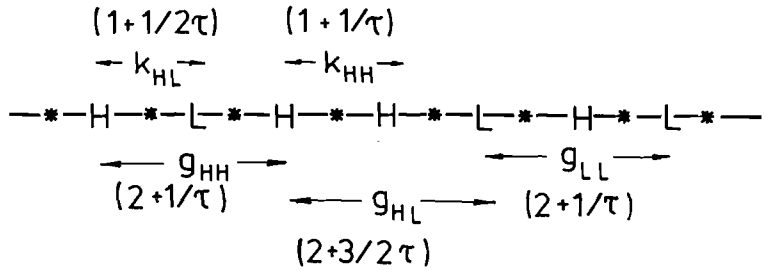

Fig.1. The model of NN (k_{HL},k_{HH}) and NNN (g_{HH},g_{HL},g_{LL}) interactions of atoms in the harmonic model of 1D QBA.

presented in Fig.1,where the asterisks (*) indicate the points of 1D QL (4); the letters H and L denote atoms whose masses are $M_0(1+q)$ and M_0,respectively, and the dimensionless distances between the atoms are given in parantheses.

In this paper the one-dimensional harmonic model of lattice dynamics of binary alloy with quasiperiodic distribution of masses (5) but constant isotropic forces

$$k_{HL} = k_{HH} = k_0 \qquad (7)$$

$$g_{HL} = g_{HH} = g_{LL} = k_0 \qquad (8)$$

is studied; k_0 and g_0 are the force constants of NN and NNN interactions, respectively.

3. Basic equations

We take the Hamiltonian of the system in the form

$$H = \sum_{l=1}^{N} \frac{P_l^2}{2 M_l} + \frac{1}{2} \sum_{l=1}^{N} k_0 (u_l - u_{l+1})^2 + \frac{1}{2} \sum_{l=1}^{N} g_0 (u_l - u_{l+2})^2 , \quad (9)$$

where P_l and u_l are the momentum and displacement of l-th atom with the mass $M_l = M_0 (1 + q ([(l+1)/\tau] - [l/\tau]))$, respectively.

The system of equations of motion is

$$M_l \ddot{u}_l = k_0 (u_{l+1} + u_{l-1} - 2 u_l) + g_0 (u_{l+2} + u_{l-2} - 2 u_l) \quad (10),$$
$$l = 1, \ldots, N$$

Now we introduce the new variables $u_l(t) = \sqrt{m_l}\, Q_l(t)$ and assume that dependence of Q_l on time has the form [6]

$$Q_l(t) = Q_l^0 \exp (i \omega_0 t). \quad (11).$$

Then the system (10) can be rewritten as follows

$$\Omega^2 Q_l = \alpha_l Q_l + \beta_{l-1} Q_{l-1} + \beta_{l+1} Q_{l+1} + \gamma_{l-2} Q_{l-2} + \gamma_{l+2} Q_{l+2} , \quad (12)$$
$$l = 1, \ldots, N$$

where Ω denotes the dimensionless eigenfrequency $\Omega = \omega_0 \sqrt{M_0/k_0}$ and

$$\alpha_l = 2 \frac{M_0}{M_l} (1 + h) \quad (13a)$$

$$\beta_{l+1} = - M_0 / \sqrt{M_l M_{l+1}} \quad (13b)$$

$$\gamma_{l+2} = - h M_0 / \sqrt{M_l M_{l+2}} , \quad (13c)$$
$$l = 1, \ldots, N$$

where $h = g_0/k_0$ defines the strength of NNN interactions.

The sequence (13a) takes two values: $\alpha^{(1)} = 2 (1+h) / (1+q)$ and $\alpha^{(2)} = 2(1+h)$. For a given N the average numbers $n(\alpha^{(1)})$ and $n(\alpha^{(2)})$ of $\alpha^{(1)}$ and $\alpha^{(2)}$ terms in $\{\alpha_l\}$ are $[N/\tau]$ and $[(1-1/\tau)N]$, respectively.

The binary sequence (13b) is a successor of (13a) [7,8] since it can be obtained from $\{\beta_{l+1}\}$ by means of the substitution rule

$$\alpha^{(1)} \to \beta^{(2)}\beta^{(2)}$$

$$\alpha^{(2)} \to \beta^{(1)} , \quad (14)$$

where $\beta^{(2)} = -1 / \sqrt{1 + q}$ and $\beta^{(1)} = - 1 / (1 + q)$.
We point out that the $\beta^{(1)}$ elements appear always isolated and the $\beta^{(2)}$ elements occur in a string of 2 or 4 consecutive elements in the sequence (13b). Therefore in $\{ \beta_{l+1} \}$ there are on average $2N/(\tau+1)$ and $N/(2\tau+1)$ elements of $\beta^{(2)}$ and $\beta^{(1)}$, respectively.

The sequence (13c) takes three values: $\gamma^{(1)} = - h/(1+q)$, $\gamma^{(2)} = - h$, $\gamma^{(3)} = -h / \sqrt{1 + q}$. We note that $\{ \gamma_{l+2} \}$ can be obtained from $\{ \beta_{l+1} \}$ with the help of the substitution rule

$$\beta^{(2)}\beta^{(2)}\beta^{(1)} \to \gamma^{(1)}\gamma^{(3)}\gamma^{(3)}$$

$$\beta^{(2)}\beta^{(2)}\beta^{(2)}\beta^{(2)}\beta^{(1)} \to \gamma^{(1)}\gamma^{(2)}\gamma^{(1)}\gamma^{(3)}\gamma^{(3)} . \quad (15).$$

Taking into consideration the above-mentioned properties of the sequences (13) one can show that for $N \gg 1$ in (13c) there are on average $[N/\tau^2]$, $[2N/\tau^3]$ and $[N/\tau^4]$ of $\gamma^{(1)}$, $\gamma^{(2)}$ and $\gamma^{(3)}$ terms, respectively (see Appendix A).

The frequencies Ω of normal vibrations of 1D QBA are the eigenvalues of the N*N symmetric band matrix (cf. Eqs.12) if the FEBC are used [1]. Note that in this case, (13b) and (13c) define the off-diagonal elements of the dynamical matrix (DM) for $1 \le l \le N-1$ and $1 \le l \le N-2$, respectively; $\beta_1 = \gamma_1 = \gamma_2 = 0$. The relations (13a) give the values of α_l for $3 \le l \le N-2$ and $\alpha_1 = M_0 (1 + h)/M_1$, $\alpha_2 = M_0 (2 + h)/M_2$, $\alpha_{N-1} = M_0(2 + h)/ M_{N-1}$, $\alpha_N = M_0 (1 + h)/ M_N$.

4. The numerical results

The integrated density of states (IDOS) G(x), its histograms $\Delta G(x)$ and the density of states (DOS) $\rho(y)$ have been calculated for various values of model parameters q and h. The computer simulations have been done for a large chain with $N \le 10^5$ atoms under FEBC using Dean's method [1,6].

Let us note that: (1) G(x) determines the number of eigenfrequencies (EF) Ω_i of DM fulfilling the condition: $\Omega_i^2 < x$, where $x = \Omega^2 = M_0\omega_0^2/k_0$; (2) the function $\Delta G(x) = G(x) - G(x - \Delta)$ gives the number of EF in the interval $(x-\Delta , x)$, where Δ denotes an elementary step of calculations; (3) DOS $\rho (y)$ is defined by

$$\rho (y) = \frac{G_1(y) - G_1(y - \Delta_1)}{N \Delta_1} . \qquad (16)$$

where $y = \sqrt{x / x_{max}}$, Δ_1 denotes the step of calculations of the function G_1 that determines the number of EF of DM obeying the condition $\Omega_i < y$.

The numerical results for h = 0 and increasing values of POQ and for $q = 1/\tau$, $h > 0$ are presented in Figs.2-4 and in Figs.5,6,

respectively. Note that in Figs.3-6 on the abscissa axes the values of $X_{RED} = x / x_{max} = \Omega^2 / \Omega^2_{max}$ are depicted, where Ω_{max} denotes the maximal dimensionless eigenfrequency of DM. In addition , N_i define the number of states in distinguishable (at the used scale and magnitude of Δ) "subbands"; in Fig.3b $N_9=2N_2=18024$; in Fig.3c (z=1.0) the "subbands" numerated by index i of N_i contain the following number of EF: $1\equiv N_1=23608$, $2\equiv N_2=14589$, $3\equiv 10\equiv N_3=N_{10}=9017$, $4\equiv N_4=5573$, $5\equiv 8\equiv N_5=N_8=3444$, $6\equiv 7\equiv N_6=N_7=N_4$, $9\equiv 11\equiv N_9=N_{11}=N_4-1$ and $12\equiv N_{12}=N_3+1$.

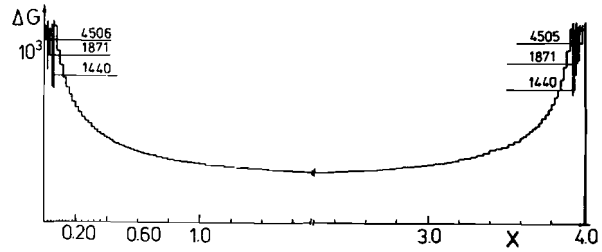

Fig.2. The histogram ΔG as a function of $x=\Omega^2=M_0\omega_0^2/k_0$; q= 0 (the ideal periodic chain), h=0.0, $N=10^5$. The step of calculations Δ = 0.02; the numbers of EF are depicted in the acoustic and optical part of the spectrum.

The substructures of ΔG for a decreasing magnitude of the step of calculations Δ are presented in Figs.7,8 and in Figs. 9-11 in the acoustic and optical regions of VS, respectively.

The dependence of ρ on y (cf. Eq.(16)) is shown in Figs. 12a, 12b, and 12c for $q= 1/\tau$ (h=0.0), $q= 10/\tau$ (h = 0.0) and $q = 1/\tau$, , h= 0.25, respectively. Note that $\Delta=\Delta_1= 1/225$, and the values of $\log_{10}(\rho)$ less than 10^{-2} represent the isolated states in the gaps.

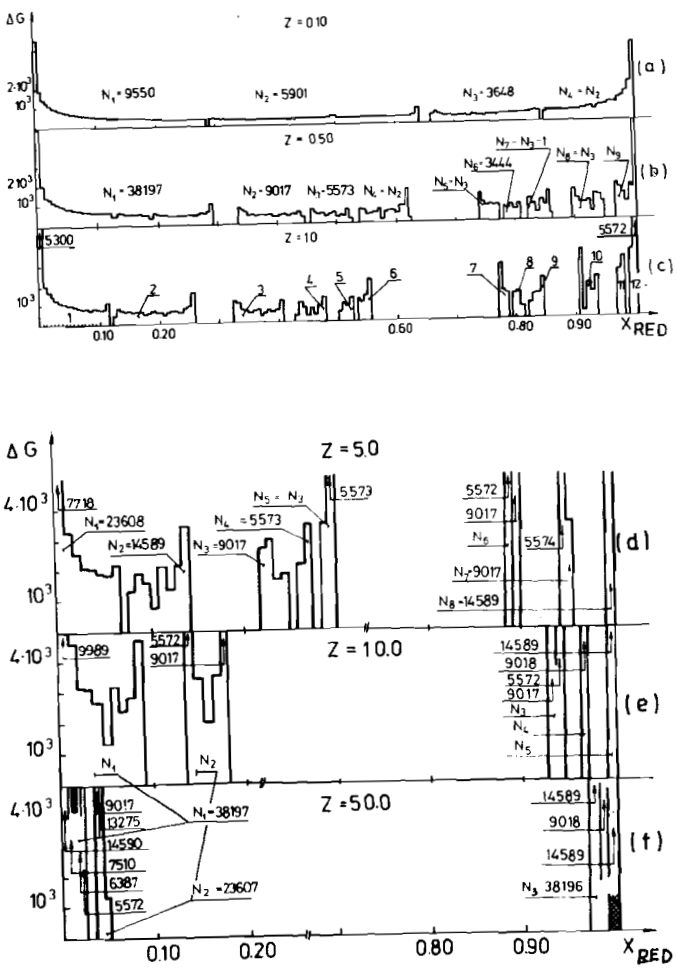

Fig.3. ΔG versus $X_{RED} = \Omega^2/\Omega^2_{max} = x/x_{max}$ where Ω_{max} is the maximal eigenfrequency of DM; $q = z/\tau$. In Fig.3a and in Figs.3b-3f the total number of atoms is $2.5*10^4$ and 10^5, respectively.

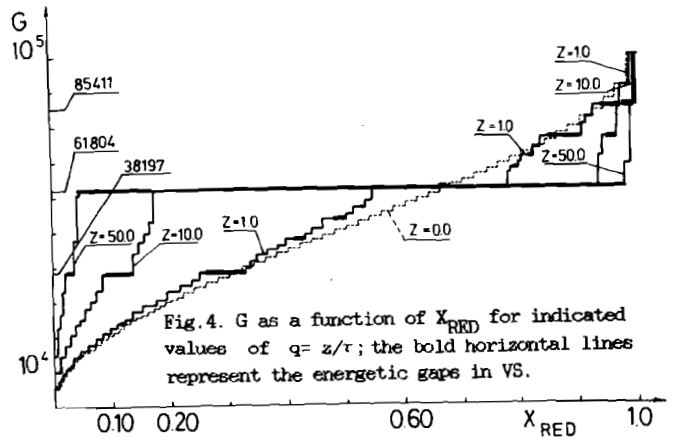

Fig.4. G as a function of X_{RED} for indicated values of $q = z/\tau$; the bold horizontal lines represent the energetic gaps in VS.

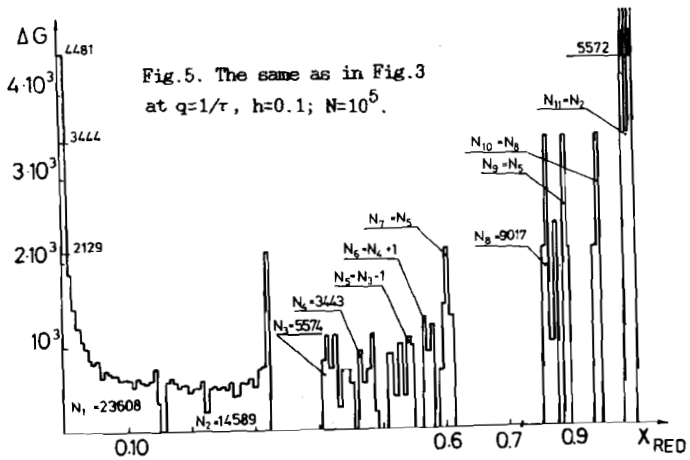

Fig.5. The same as in Fig.3 at $q=1/\tau$, $h=0.1$; $N=10^5$.

The dependences of $\rho(y=\Delta_1=1/225)=\rho_1$ on q at $h=0.0$ and ρ_1 on h at $q = 1/\tau$ are presented in Figs.13a and 13b, respectively. In Fig.13a the values of ρ_1 obtained in the framework of the model studied in I are depicted by squares.

In order to study the substructure of VS the dynamical matrix has been diagonalized [1]. Computations have been performed for an increasing number of atoms N in the chain. The results for F_{10}

$=55 \le N \le F_{16}=987$, $q=1/\tau$, $h=0.0$ and $q=1/\tau$, $h=0.25$ are presented in Figs.14 and 15, respectively.

Analysing the VS we have obeserved that in the acoustic region the EF of DM are given within 3% by (see also Ref. [1])

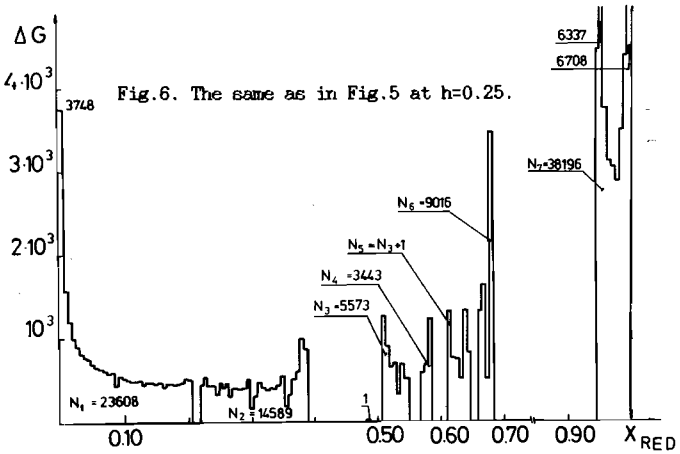

Fig.6. The same as in Fig.5 at h=0.25.

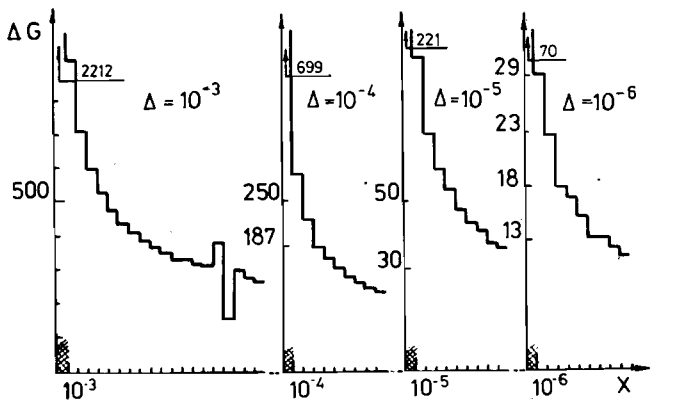

Fig.7. ΔG versus x in the acoustic region of VS for decreasing values of Δ; $q=10/\tau$, $N=10^5$, h=0.0.

$$\Omega_i\ (\ q,h\ ) = 2\ \Gamma_i\ (q,h)\ \sin\ ((i-1)\pi/2N) \simeq$$

$$\simeq 2\ \Gamma_2\ (q,h)\ \sin\ ((i-1)\pi/2N) \qquad (17)$$

$$1 \le i \le [N/\tau^5]\ ,$$

where $\Gamma_i = \Omega_i\ (\ q,h\ )\ /\ \Omega_i(\ q=0,h=0)$.

We have calculated the dependences of $\Gamma_2(\ q\ ,\ h\ )$ on q at h=0 and on h for fixed q. The results are shown in Fig.16.

In addition, the fractal dimension $\bar{d}$ of VS has been computed using Mandelbrot's covering methods [1,9]. We have determined $\bar{d}$ within 1% and 10% for $q \lesssim 1$ and $q \gtrsim 10^2$, respectively. The dependences of $\bar{d}$ on q at h=0.0 and on h at $q=1/\tau$ are shown in Fig.17.

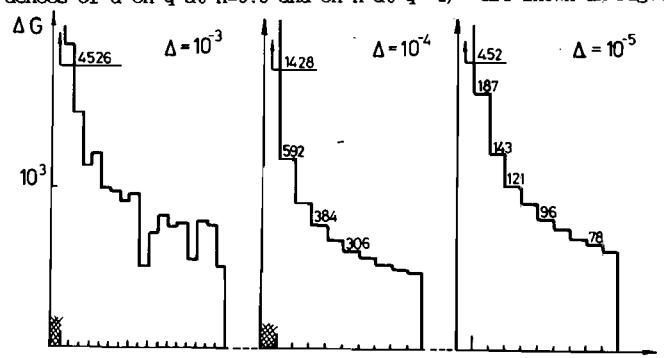

Fig.8. The same as in Fig.7 at $q=50/\tau$.

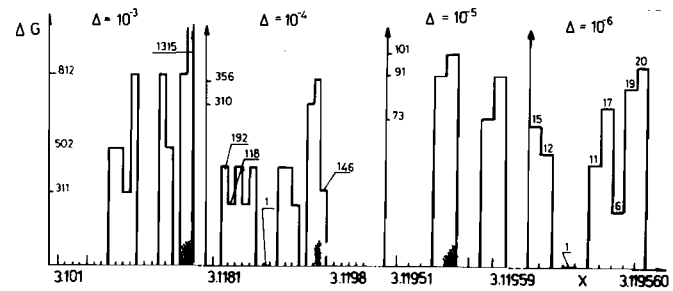

Fig.9. ΔG as a function of x in the optical region of VS for decreasing Δ ; $q=1.0/\tau$, h=0.0, $N=10^5$.

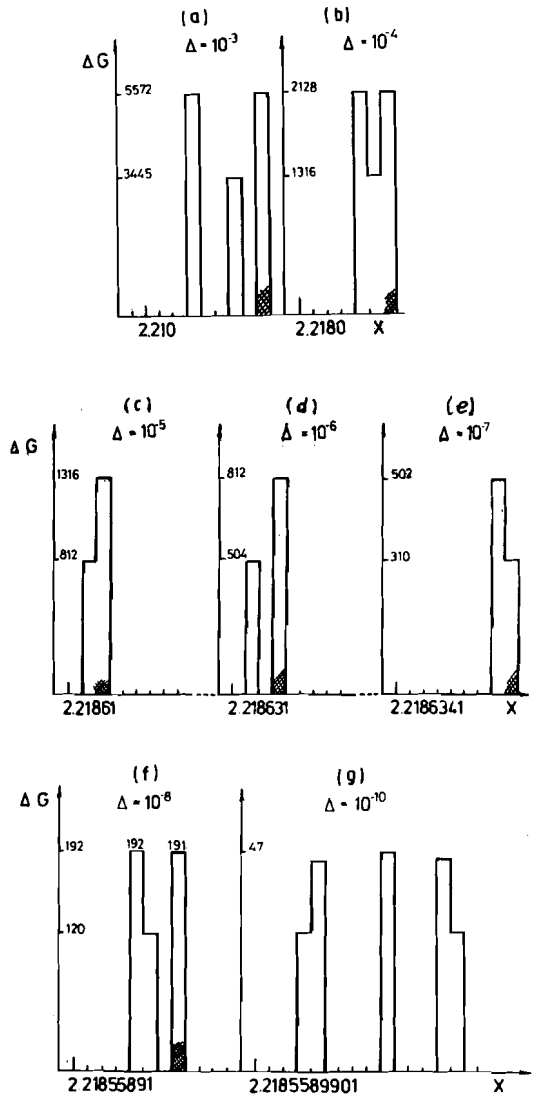

Fig.10. The same as in Fig.9 at $q=10/\tau$.

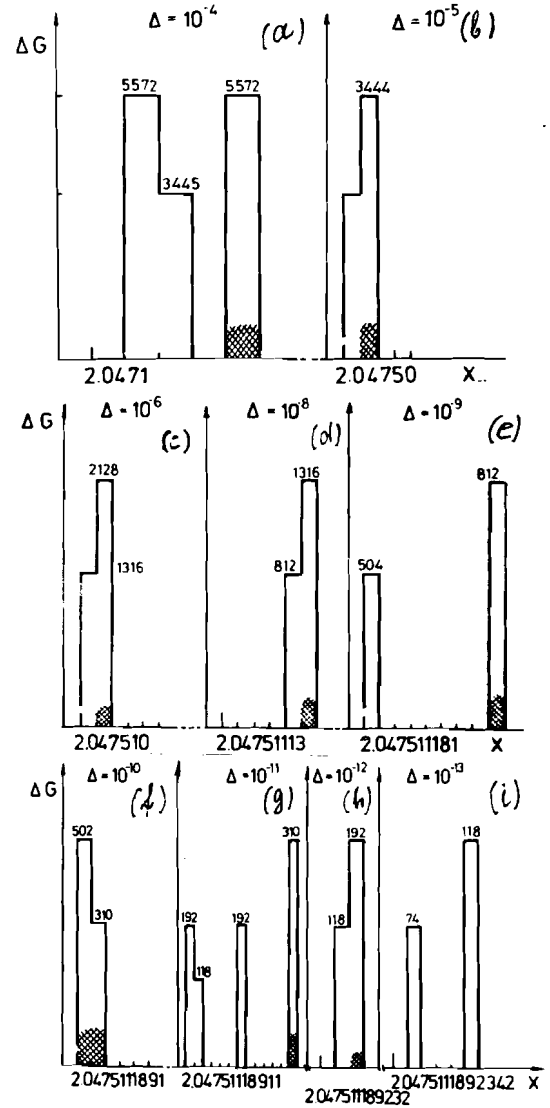

Fig.11. The same as in Fig.9 at $q=50/\tau$.

5. Conclusions

One can draw the following conclusions from the numerical results presented in this paper.

1. Vibrational spectra of 1D QBA have the substructure of the Cantor-set-type (cf.Figs.3-6, 9-12 ,14,15) which can be described as follows. At the given magnitute of the step of calculations $\Delta = \Delta_1$ (which can be interpreted as the smallest value of the distinguishable gap) we observe that in VS there exists a finite number of "subbands " $\{ E_1, E_2, \ldots, E_m \}$ containing $\{ n(E_1), n(E_2), \ldots, n(E_m) \}$ number of EF and each $n(E_i)$ is given by $[N(1-1/\tau)^k / \tau^l]$ where $k > 0$, $l > 0$ are the natural numbers (cf. Figs. 3-6,14, 15). If Δ is decreasing, then the spectrum $\{ E_1, E_2, \ldots, E_m \}$ is splitting into narrower "subbands" $\{ E'_1, E'_2, \ldots, E'_{m_1} \}$, $m_1 > m$ in the following way: the given "subband" E_i with $n(E_i)$ eigenstates (at $\Delta=\Delta_1$) is branching, at sufficiently small $\Delta=\Delta_2 < \Delta_1$, into two "subbands" having $n(E'_i)$ and $n(E'_{i+1})$ EF and $n(E'_i) / n(E'_{i+1}) = \tau$. If $\Delta = \Delta_3 < \Delta_2$ is decreasing further, then the new "subband" structure, with the gaps the widths of which are greater than Δ_3, emerges and so on (cf. Figs.9-12).

One can expect that the vibrational spectrum of the infinite 1D QBA is the singular continuous one [10,11], i.e., the energetic gaps are densely distributed in the phonon spectrum.

2. The above described Cantor-set-like structure of VS almost completely disappears in the acoustic region (cf. Figs.3-8,13,16) and manifests itself in the optical region (cf. Figs.3-6,9-12,14, 15).

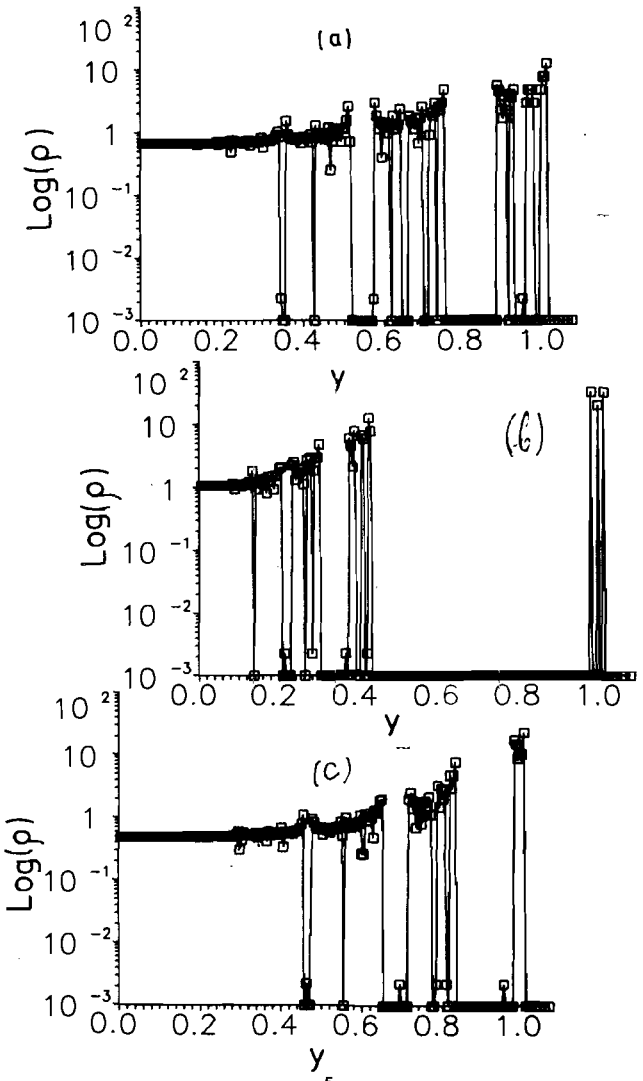

Fig.12. $\mathrm{Log}_{10}(\rho)$ versus y, $N = 10^5$; (a) $q = 1/\tau$, $h = 0$; (b) $q = 10/\tau$, $h=0$; (c) $q=1/\tau$, $h=0.25$; $\rho=0$ is depicted as $\rho=10^{-3}$.

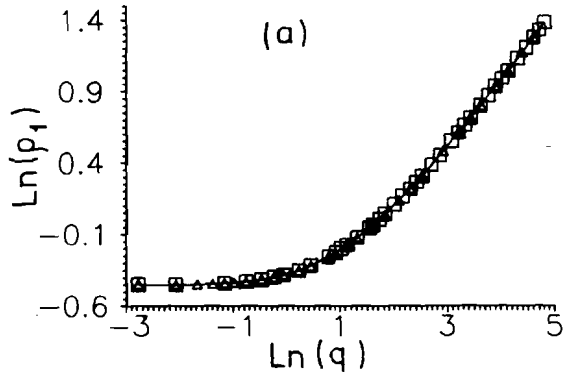

Fig.13a. Ln(ρ(y=1/225)) versus ln(q); the squares and triangles represent the values obtained within the model considered in I and in the present paper, respectively.

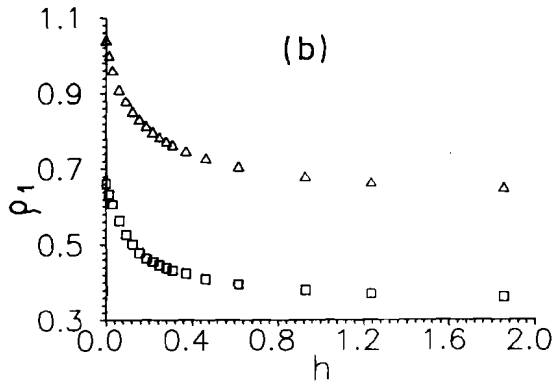

Fig.13b. $\rho(\Delta_1=1/225)$ versus h; $q=1/\tau$, $N=10^5$.

3. The vibrational spectra are self-similar and this feature allows us to calculate their fractal dimension using Mandelbrot's method [9]. The fractal dimension $\bar{d}$ shows a power-decay if the parameter of quasiperiodicity q is growing up [1,12]. The fit of

the function q^{α} to the numerical results (cf.Fig. 17) at $q \geq 0.5/\tau$ gives

$$\bar{d} = C\, q^{\alpha}, \qquad (18)$$

where $\alpha = -$ (0.11 ± 0.02) and C = 0.83 ± 0.04 (see also Ref. [1]).

4. The width Δ_g of the gap is an increasing function of q (cf. Figs.3,4,12a,12b). In other words, the distances between EF of DM decrease if POQ is growing up (cf.Figs.9-11). This implies that

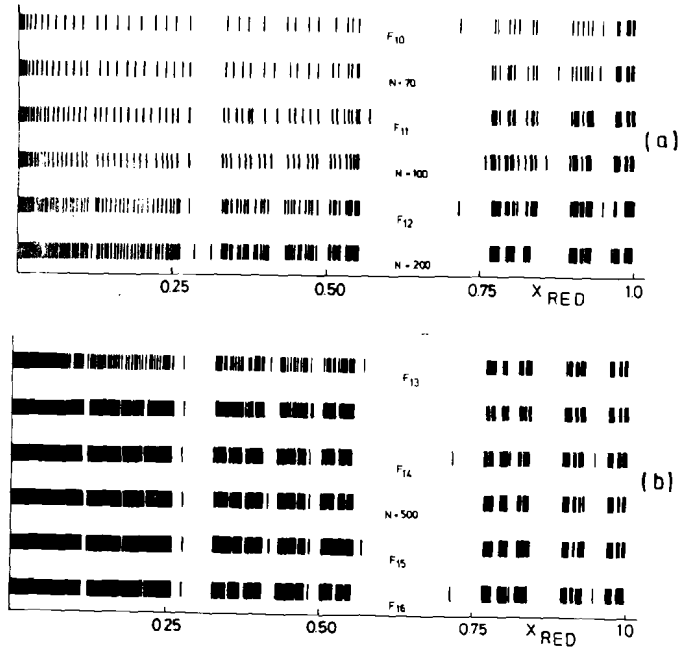

Fig.14. VS for the increasing number N; q= $1/\tau$, h= 0.0; F_{10}= 55, F_{11}=89 and $F_i=F_{i-1} + F_{i-2}$. On the abscissa axis X_{RED} is depicted.

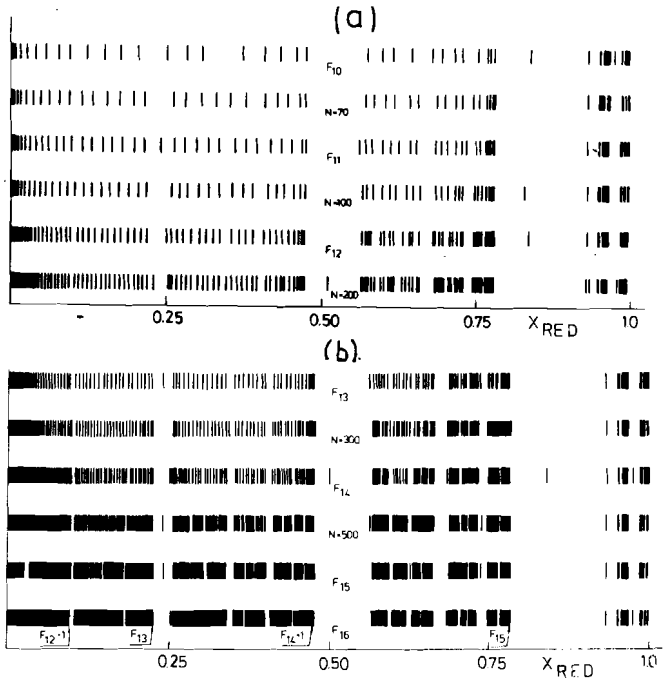

Fig.15. The same as in Fig.14 at h=0.25.

the graphis of the functions ΔG as well as ρ become more narrower and higher as q is increasing (cf.Figs.3,12a,12b). In addition, Δ_g tends to zero in short- and long-wavelength limits.

5. If one neglects the energetic gaps whose widths are less than the given real number Δ_0, then the phonon spectra are "band-like" and the functions ΔG and ρ exhibit characterictic singularities (described below) of the ideal periodic chain (cf. Fig. 2) near the edges of each "subband".

5.1. In the acoustic region ($x \ll 1$) the phonon spectra have almost continuous character (cf.Figs.3,4,7,8,12,16). Eigenfrequences of DM are given by formula (17) (cf.Fig.16) describing the distribution of eigenenergies in the phonon spectrum of an ideal chain. For this reason one observes that:

5.1.1. The dependences of ΔG on x show the Van Hove singularities as $x \longrightarrow 0$ i.e., $\Delta G(q,h,x) \underset{x \longrightarrow 0}{=} \Delta G_0(q,h)/\sqrt{x}$ [13] (cf.Figs.3,5-8).

5.1.2. If $y \longrightarrow 0$, then the density of states ρ (y) tends to a constant value C_1 depending on q and h (cf.Figs.12a,12b).

5.2. The function ΔG(x) (as well as $\rho(y)$) increases remarkably at the upper edge of each "subband" (cf.Figs.3,5,6,12). This reflects the Van Hove singularity $\Delta G(q,h,x) \underset{x \longrightarrow x_{max}}{=} \Delta G_0'(q,h) / \sqrt{x_{max} - x}$ of the periodic chain [13] (cf.Fig.2).

6. The vibrational spectra of 1D QBA show characteristic tendencies if the model parameter h increases:

6.1. The density of states ρ decreases in the acoustic region and the peaks of ΔG become higher in the optical region (cf. Figs. 5,6; compare Fig.12a and Fig.12c).

6.2. The width of energetic gaps decreases (compare Fig.3c and Figs.5,6).

6.3. The fractal dimension $\bar{d}$ of the phonon spectra enlarges (cf. Fig.17b).

7. As a consequence of the applied free end boundary condition (simulating the surfaces of the chain), VS exhibit the eigenstates inside some gaps (cf.Figs.12,14,15). The eigenvectors corresponding to these EF are localized at the ends of the chain [14].

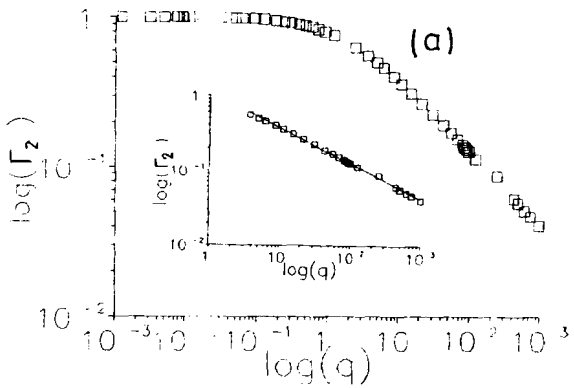

Fig.16a. Dependence of $\log_{10}(\Gamma_2(q,h=0))$ on log (q); $N=F_{17}=1597$. Inset shows the power dependence of Γ_2 on q for $q \gg 1$. The best fit is given by $\Gamma_2 = (1.1 \pm .05) * q^{-(0.47 \pm .02)}$.

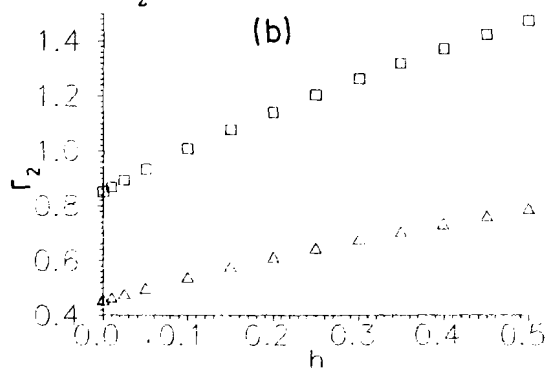

Fig.16b. $\Gamma_2(q,h)=\Omega_2(q,h)/\Omega_2(0,0)$ versus h, $N=F_{17}$; squares and triangles correspond to $q=1/\tau$ and $q=10/\tau$, respectively.

8. If h=0.0, then the model under consideration leads to the same qualitative results as the model studied in I (cf. Figs. 13a). But for $h \neq 0$ these models are nonequivalent since they have a

different number of the diagonal ($\{\alpha_1\}$) and off-diagonal ($\{\gamma_{1+2}\}$) elements of the dynamical matrix.

Finally, let us note that in the accoustic region the vibrational spectrum of 1D QBA looks like the spectrum of the ideal periodic chain. For this reason, the thermodynamic properties of the periodic and quasiperiodic chains should coincide. Our studies of the temperature dependence of the heat capacity [15 ,16] confirm this expectation.

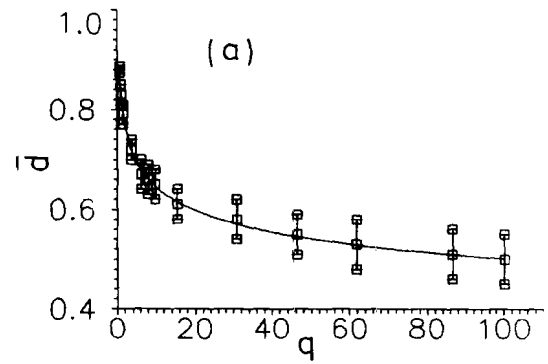

Fig.17a. The fractal dimension $\bar{d}$ of $(\Omega^2_{min}, \Omega^2_{max})$ versus q at $N=F_{19}=4181$. The solid line is the power function $\bar{d} = 0.83 * q^{-0.11}$.

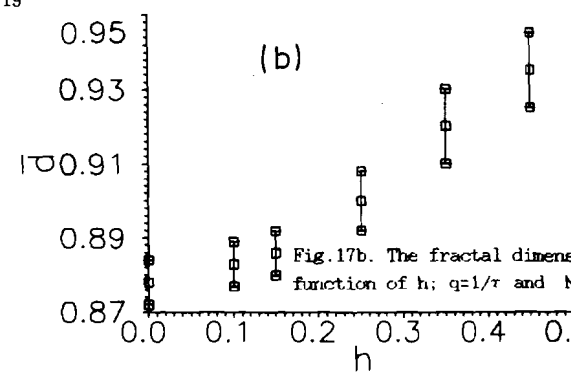

Fig.17b. The fractal dimension $\bar{d}$ as a function of h; $q=1/\tau$ and $N=F_{19}$.

Recently, we have studied the properties of the eigenvectors of the dynamical matrix, and the obtained results [14] agree with above conclusions.

Appendix A.

Let $n_1(\gamma^{(1)}), n_2(\gamma^{(2)})$ and $n_3(\gamma^{(3)})$ denote the number of $\gamma^{(1)}$, $\gamma^{(2)}$ and $\gamma^{(3)}$ terms in N_1 consecutive elements of the sequence (13c). Below, we shall calculate the ratios

$$r_i(\gamma^{(i)}) = \frac{n_i(\gamma^{(i)})}{N_1} \qquad i = 1,2,3 \qquad (A1)$$

for $N_1 \gg 1$.

We note that

P1. The sequence (13b) is a successor of (13a) (see the substitution rule (14) in Sec.3);

P2. The sequence (13c) is a successor of (13b) (see the substitution rule (15) in Sec.3);

P3. From P1 it follows that N elements of (13a) give $N(1+1/\tau)$ elements of (13b).

Now we shall calculate the ratio $r_2(\gamma^{(2)})$. The number $n_2(\gamma^{(2)})$ is equal to the number N_0 of $\beta^{(2)}\beta^{(2)}\beta^{(2)}\beta^{(2)}\beta^{(1)}$ terms in (13b) (property P2). On the other hand, N_0 determines the number of $\alpha^{(1)}\alpha^{(1)}$ pairs in (13a) (property P1). So for $N \gg 1$ we have

$$N_0 = N - 1 - 2(1 - 1/\tau)N \cong (2/\tau - 1)N, \qquad (A2)$$

where $2(1-1/\tau)N$ gives the number of $\alpha^{(1)}\alpha^{(2)}$ and $\alpha^{(2)}\alpha^{(1)}$ pairs in (13a) and from here

$$r_2(\gamma^{(2)}) = \frac{N_0}{N(1+1/\tau)} = 1/\tau^4. \qquad (A3).$$

We shall further calculate the ratio $r_3(\gamma^{(3)})$. Note that $\beta^{(2)}\beta^{(1)}$ term of $\{\beta_{l+1}\}$ gives $\gamma^{(3)}\gamma^{(3)}$ term in $\{\gamma_{l+2}\}$ (property P2). For this reason

$$n_3(\gamma^{(3)}) = 2\, n(\beta^{(1)}), \qquad (A4)$$

where $n(\beta^{(1)})$ is the number of $\beta^{(1)}$ terms in $\{\beta_{l+1}\}$. But $n(\beta^{(1)})$ is equal to the number $n(\alpha^{(2)}) = N(1 - 1/\tau)$ of $\alpha^{(2)}$ terms in N consecutive elements of $\{\alpha_l\}$ (property P1). Hence

$$r_3(\gamma^{(3)}) = \frac{n(\alpha^{(2)})}{N(1 + 1/\tau)} = 2/\tau^3 \qquad (A4)$$

and finally

$$r_1(\gamma^{(1)}) = 1 - r_2(\gamma^{(2)}) - r_3(\gamma^{(3)}) = 1/\tau^2. \qquad (A5).$$

Acknowledgments

The author is thankful to Prof. N.M.Plakida for usuful remarks and to Dr. J.Malek for the assistance in preparation of the numerical programs. Computations have been done at the Laboratory of Computing Techniques and Automation of the Joint Institute for Nuclear Research.

References

1.W.Salejda, "The Vibrational Spectra of the One-Dimensional Fibonacci-Type Quasicrystals"; Preprint of JINR, E17-89-281, Dubna 1989 (submitted to Acta Physica Polonica).

2.S.E.Burkov, J. Stat. Phys. 47 , 409 (1987).

3.D.Levine, P.J.Steinhardt, Phys. Rev. Lett. 53, 2477 (1984).

4.D.Levine, P.J.Steinhardt, Phys. Rev. B34, 596 (1986).

5.J.E.S.Socolar, P.J.Steinhardt, ibid., B34, 617 (1986).

6.P.Dean, Rev. Mod. Phys. 44, 127 (1972).

7.I.Aviram, J.Phys. A19, 3299 (1986).

8.I.Aviram, ibid.,A20, 1025 (1987).

9.B.B.Mandelbrot, "The Fractal Geometry of Nature", W.H.Freeman Company, New York 1983; Chap.6.

10.M.Reed, B.Simon, "Methods of Modern Mathematical Physics,1, Functional Analysis", Academic Press, New York, 1975; Chap.7.

11.S.Ostlund, R.Pandit, Phys. Rev., B29, 1394 (1986).

12.M.C.Valsakumar, G.Ananthahrishna, J.Phys. C20, 9 (1987).

13.N.W.Ashcroft, N.D.Mermin, "Solid State Physics", Holt,Rinehart and Winston, New York, 1983.

14.W.Salejda, in preparation.

15.W.Salejda, Communication of JINR, E17-88-880, Dubna 1988.

16.W.Salejda, Preprint of JINR, E17-88-881, Dubna 1988; to be published in International Journal of Modern Physics B (1989).

Received by Publishing Department
on Jule 17, 1989.

Салейда В.
E17-89-538

Колебательные спектры одномерной гармонической модели квазипериодического бинарного сплава

Численными методами исследуется динамика решетки гармонической модели одномерного квазипериодического бинарного сплава. Взаимодействие ближайших и следующих соседей задано при помощи постоянных силовых констант. Распределение атомов вдоль цепочки определяет бинарная квазипериодическая последовательность. С применением метода Дина и свободных граничных условий вычислена интегральная плотность состояния G, ее гистограммы ΔG и функция плотности фононных состояний ρ для больших цепочек, содержащих $N = 10^5$ атомов. Исследовано влияние изменения параметров модели на G, ΔG и ρ. Описана субструктура колебательных спектров (КС), имеющих структуру канторова множества. Вычислена фрактальная размерность $\bar{d}$ КС для цепочек с $N = F_{19} = 4181$ числом атомов. Показано, что (1) $\bar{d}$ падает степенным образом при увеличении так называемого параметра квазипериодичности и (2) $\bar{d}$ растет при увеличении силы взаимодействия следующих соседей.

Работа выполнена в Лаборатории теоретической физики ОИЯИ.

Препринт Объединенного института ядерных исследований. Дубна 1989

Salejda W.
E17-89-538

The Vibrational Spectra of the One-Dimensional Harmonic Model of the Quasiperiodic Binary Alloy

The lattice dynamics of the harmonic model of the one-dimensional quasiperiodic binary alloy is studied numericaly. It is assumed that the nearest-neighbour and next-nearest-neighbour interactions (NNN) of atoms are given by constant isotropic forces. The distribution of the masses of atoms along the chain defines the binary quasiperiodic sequence. The integrated density of states G, its histograms ΔG and the density of states ρ are calculated using Dean's algorithm under free-end boundary conditions for large chains with 10^5 atoms. The effects of variation of the model parameters on G, ΔG and ρ are studied. The Cantor-set-type structure of vibrational spectra (VS) is describe. The fractal dimension $\bar{d}$ of VS is calculated for the chains with N = 4181 atoms. It is established that: (1) $\bar{d}$ shows a power-law decay if the so-called parameter of quasiperiodicity is increasing and (2) if the strength of NNN interactions increases, then $\bar{d}$ grows up.

The investigation has been performed at the Laboratory of Theoretical Physics, JINR.

Preprint of the Joint Institute for Nuclear Research, Dubna 1989